Chemistry & Biology
Article

Targeting a Prokaryotic Protein in a Eukaryotic Pathogen: Identification of Lead Compounds against Cryptosporidiosis

Nwakaso N. Umejiego,[1,2] Deviprasad Gollapalli,[1] Lisa Sharling,[2] Anna Volftsun,[3] Jennifer Lu,[1] Nicole N. Benjamin,[3] Adam H. Stroupe,[2] Thomas V. Riera,[1] Boris Striepen,[2] and Lizbeth Hedstrom[1,3,*]
[1]Department of Biochemistry, Brandeis University, 415 South Street, Waltham, MA 02454, USA
[2]Center for Tropical and Emerging Global Diseases and Department of Cellular Biology, University of Georgia, 500 D.W. Brooks Drive, Athens, GA 30602, USA
[3]Department of Chemistry, Brandeis University, 415 South Street, Waltham, MA 02454, USA
*Correspondence: hedstrom@brandeis.edu
DOI 10.1016/j.chembiol.2007.12.010

SUMMARY

Cryptosporidium parvum **is an important human pathogen and potential bioterrorism agent. No vaccines exist against *C. parvum*, the drugs currently approved to treat cryptosporidiosis are ineffective, and drug discovery is challenging because the parasite cannot be maintained continuously in cell culture. Mining the sequence of the *C. parvum* genome has revealed that the only route to guanine nucleotides is via inosine-5′-monophosphate dehydrogenase (IMPDH). Moreover, phylogenetic analysis suggests that the IMPDH gene was obtained from bacteria by lateral gene transfer. Here we exploit the unexpected evolutionary divergence of parasite and host enzymes by designing a high-throughput screen to target the most diverged portion of the IMPDH active site. We have identified four parasite-selective IMPDH inhibitors that display antiparasitic activity with greater potency than paromomycin, the current gold standard for anticryptosporidial activity.**

INTRODUCTION

The "vicious cycle of diarrhea and malnutrition" in developing countries could be broken with the advent of effective chemotherapy against *Cryptosporidium parvum* (Berkman et al., 2002; Huang et al., 2004; Huang and White, 2006). *C. parvum* is also an important pathogen in the developed world, where AIDS patients are at risk of severe infection (Carey et al., 2004; Fayer, 2004). The parasite produces spore-like oocysts that are resistant to common methods of water treatment, so *Cryptosporidium* also poses a credible bioterrorism threat (DuPont et al., 1995). The tools to respond to such an incident are woefully inadequate: no vaccines or effective drug treatments are currently available. The damage would be substantial: the economic cost of the 1993 Milwaukee outbreak, where ~400,000 individuals contracted disease, totaled $31.7 million in medical costs and another $64.6 million in productivity losses (Corso et al., 2003). Independent of such bioterrorism scenarios, effective drugs are urgently needed for the management of cryptosporidiosis in AIDS patients and epidemic outbreaks.

The search for drugs to treat cryptosporidiosis has been almost futile. Compounds such as spiramycin, clarithromycin, paromomycin, and nitazoxanide display modest activity in model systems but limited efficacy in clinical trials with immunocompetent patients and poor efficacy in immunocompromised patients (Abubakar et al., 2007; Mead, 2002). Commonly used antiparasitic drugs fail against *C. parvum*, which is not surprising given that the *C. parvum* genome has undergone massive gene loss and horizontal transfer when compared with related apicomplexan parasites such as *Plasmodium* and *Toxoplasma* (Abrahamsen et al., 2004; Striepen et al., 2004; Templeton et al., 2004; Xu et al., 2004). *C. parvum* cannot be maintained in continuous cell culture and genetic tools do not exist, so the validation of new drug targets is thwarted by a dearth of information about parasite metabolism. Nevertheless, the *C. parvum* genome has revealed the presence of a very streamlined purine salvage pathway that relies on the uptake of adenosine (Abrahamsen et al., 2004; Striepen et al., 2004; Xu et al., 2004). The only route to guanine nucleotides is via IMPDH, which catalyzes the conversion of IMP to XMP with the concomitant reduction in NAD^+ (Figure 1A). Phylogenetic analysis suggests that *C. parvum* IMPDH was obtained from a bacterial source by lateral gene transfer (Striepen et al., 2002, 2004), and *C. parvum* IMPDH is only ~39% identical to the human isozymes IMPDH1 and IMPDH2. Whereas the IMP site is conserved, the NAD site is highly diverged and several inhibitors, most notably mycophenolic acid, bind selectively to the NAD site of human IMPDHs (Ratcliffe, 2006). Thus, the NAD site is the most promising target for parasite-selective inhibitors (Figure 1B).

Here we devise a screen to target the NAD site of *C. parvum* IMPDH and identify ten parasite-selective inhibitors with values of IC_{50} ranging from 0.1 to 20 μM. The best inhibitors display antiparasitic activity in a cell-culture model of infection. To our knowledge, these compounds are the first parasite-specific IMPDH inhibitors and the first target-based antibiotics for *C. parvum*.

RESULTS AND DISCUSSION

High-Throughput Screening

We devised an HTS to identify inhibitors that target the NAD^+ site of *C. parvum* IMPDH, taking advantage of a detailed knowledge

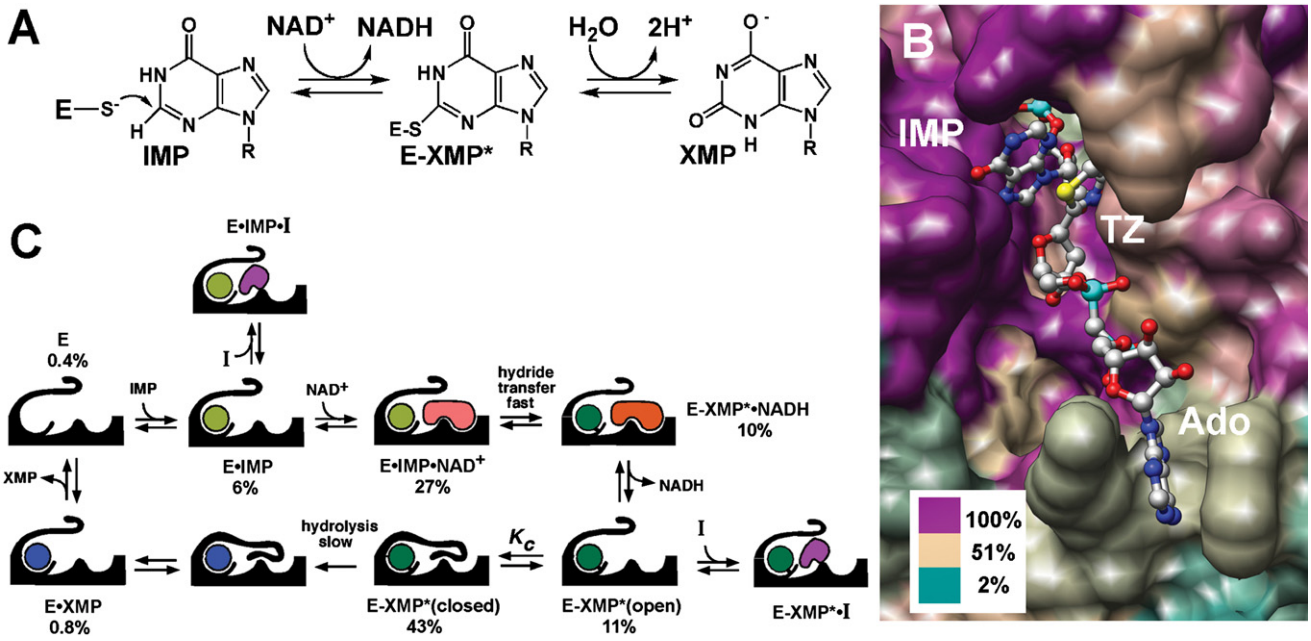

Figure 1. Mechanism and Structure of IMPDH

(A) The IMPDH reaction.

(B) The active site, rendered by sequence conservation. The structure of E•IMP•tiazofurin adenine dinucleotide complex of IMPDH from *Tritrichomonas fetus* (Protein Data Bank ID code 1LRT). The image was produced using the UCSF Chimera package (Pettersen et al., 2004). The percentage of sequence identity is colored as shown using the alignment from Striepen et al. (2002). TZ, tiazofurin; Ado, adenosine.

(C) The kinetic mechanism of IMPDH, showing the distribution of enzyme under the conditions of the HTS (250 μM IMP and 500 μM NAD^+), determined as described in the Supplemental Data. Not shown: E•NAD^+ ≤ 0.7%, E-XMP*•NAD^+ = 1%.

of the kinetic mechanism which allows us to calculate the distribution of enzyme-substrate complexes at various substrate concentrations (Figure 1C; see Table S1 in the Supplemental Data available with this article online) (Digits and Hedstrom, 1999; Umejiego et al., 2004; T.V.R., W. Wang, H. Josephine, and L.H., unpublished data). We chose high IMP concentrations (250 μM) so that IMP binds first. Under these conditions, only ~0.4% of the enzyme is in the E state and less than 0.7% will be present as E•NAD^+, so the IMP site is virtually inaccessible to inhibitors; only compounds with low nanomolar affinities for the IMP site would be identified in this screen. NAD^+ binds second and hydride transfer is rapid to form the covalent intermediate E-XMP* and NADH. NADH then departs and a mobile flap folds into the vacant site, forming the closed conformation required for the hydrolysis of E-XMP* (Hedstrom and Gan, 2006). We chose an NAD^+ concentration (500 μM) high enough to generate a robust signal in the HTS, but low enough that significant fractions of the E•IMP and E-XMP^*_{open} complexes are present (7% and 11%, respectively). Therefore, HTS should yield micromolar inhibitors that bind to the highly diverged NAD site. The HTS protocol is summarized in Table S2 and the results for a typical plate are shown in Figure S1.

This screen identified 134 compounds that inhibited *C. parvum* IMPDH by at least 45% (z scores ≤ −10; hit rate of 0.3%). Eighteen of these compounds inhibited *C. parvum* IMPDH in the secondary screen, and 11 of these 18 compounds did not inhibit human IMPDH2. Authentic samples of these compounds were purchased or synthesized, and compound structure and purity were confirmed by NMR and mass spectroscopy (see the Supplemental Data for details on synthesis). One of the authentic samples did not inhibit *C. parvum* IMPDH. The remaining 10 compounds were characterized further (compounds **A**–**K**; Table 1).

Characterization of the Principal Hits

The values of IC_{50} for these compounds range from 0.13 to 19 μM, with only compound **K** in excess of 10 μM. In all cases, the inhibition data are well described by a simple binding function (Equation S1) which indicates that the compounds are reversible inhibitors (Figure 2A). Selectivity ranges from ≥9-fold higher affinity for the parasite enzyme in the worst case (**J**) to more than 400-fold (**G**) (Table 1).

The Mechanism of Inhibition

All of the compounds are uncompetitive inhibitors with respect to IMP and noncompetitive (mixed) with respect to NAD^+ (Figures 2B and 2C), indicating that the inhibitors bind to both E•IMP and E-XMP^*_{open} as designed. Most of the compounds display similar affinities for both complexes, but **D** and **J** display a preference for E•IMP (Table 2). To further localize the site of inhibitor binding within the NAD site, we analyzed how the compounds interact with tiazofurin, which binds in the nicotinamide subsite (Hedstrom et al., 1990). Typical dual-inhibitor experiments are shown in Figures 2D–2F. If two inhibitors are mutually exclusive, a parallel line pattern is observed (Figure 2D), and α, the interaction constant, is infinity (∞). The binding of tiazofurin is mutually exclusive with all of the inhibitors, indicating that all bind in the nicotinamide subsite (**G** is too potent and **K** is too weak to permit this analysis). However, none of the inhibitors block ADP binding

Table 1. Characterization of the Parasite-Selective Inhibitors

Inhibitor	IMPDH IC_{50} (μM) *Cp*	H1[a]	H2[b]	Cp/H2	% *Cp* Growth Inhibition (SD)	Cytotoxicity (SD)	Cytostatic Effects
A 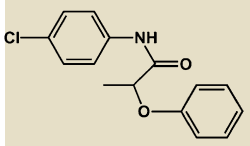	3.3 ± 0.2	>50	>50	≥15	70 (4)^{RT}	2 (6)	+
B 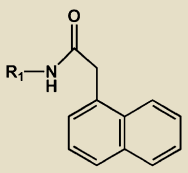	1.6 ± 0.2	>50	>50	≥30	24 (9)	49 (2)	–
C 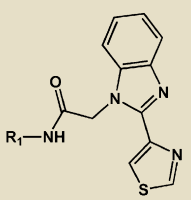	1.2 ± 0.2	>50	>50	≥40	30 (10)	n.d.	–
D 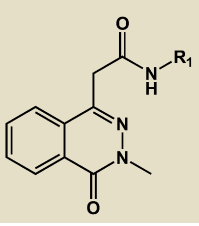	5.4 ± 0.2	>50	>50	≥10	31 (9)	n.d.	–
F 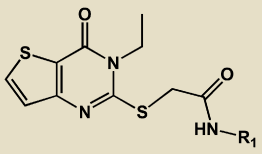	1.4 ± 0.1	>50	>50	≥35	32 (1)^{RT}	n.d.	–
G (n = 1) 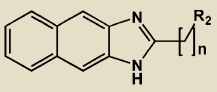	0.13 ± 0.02	>50	>50	≥400	83 (2)^{RT}	15 (5)	–
H (n = 2) 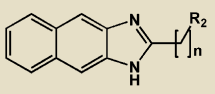	0.9 ± 0.1	>50	>50	≥50	91 (1)^{RT}	4 (2)	–
J 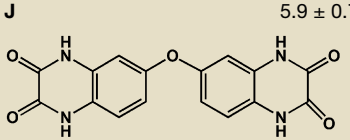	5.9 ± 0.7	>50	>50	≥9	8 (20)	7 (3)	+

Table 1. *Continued*

Inhibitor	IMPDH IC_{50} (μM)			Cp/H2	% *Cp* Growth Inhibition (SD)	Cytotoxicity (SD)	Cytostatic Effects
	Cp	H1[a]	H2[b]				
E	1.6 ± 0.2	≥25[c]	≥25[d]	≥15	20 (40)	6 (2)	–
K	19 ± 1	>500	>500	≥25	20 (60)	3 (3)	+

There is no "I." IC_{50} values are reported for enzyme inhibition. Conditions are described in Experimental Procedures. Inhibition of *C. parvum* growth was assessed in a cell-culture model using an ELISA assay or by real-time PCR (denoted with superscript RT), as described in Experimental Procedures. Cytotoxicity was assessed by measuring the release of LDH using the CytoTox assay (Promega). Cytostatic effects were evaluated with the LIVE/DEAD assay (Molecular Probes). –, no cytostatic effect; +, slightly cytostatic (<20%).

[a] Inhibition of ≤30% is observed at 50 μM inhibitor except as noted.

[b] Inhibition of ≤20% is observed at 50 μM inhibitor.

[c] Inhibition of 40% at 25 μM.

[d] Inhibition of 45% at 25 μM.

(Figures 2E and 2F; Table 2), which is somewhat surprising, as the adenosine subsite is the most different from the host enzyme (Figure 1B). Compounds **B**, **C**, **D**, **H**, and **J** interact either synergistically or independently with ADP ($\alpha \leq 1$), which indicates that the binding site for these inhibitors does not extend into the ADP subsite. In contrast, the binding of **A**, **E**, and **F** antagonizes ADP binding ($\alpha \geq 1$), indicating that the binding site for these compounds impinges on the ADP site, either directly or by inducing a conformation that decreases the affinity for ADP. Compounds **A**, **E**, and **F** are not significantly larger than the other inhibitors, which suggests that these compounds have an alternative binding mode. Thus, the screen has identified two classes of parasite-selective inhibitors.

Antiparasitic Activity in Cell-Culture Model of Parasite Growth

We next assessed whether the inhibitors have antiparasitic activity. *C. parvum* is an obligate intracellular parasite that cannot be maintained in continuous cell culture. However, sporozoites readily infect a variety of epithelial cells, undergoing the first two asexual replication cycles. Even though the life cycle is incomplete, these in vitro infections are sufficient for an initial evaluation of antiparasitic activity (Arrowood, 2002; Upton, 1997). Because parasite and host cell metabolism are intertwined, we first assessed the cytotoxic and cytostatic effects on human ileocecal adenocarcinoma epithelial HCT-8 cells, a widely used host cell model. Only compound **B** displayed significant cytotoxic effects in a lactate dehydrogenase (LDH) release assay; **G** and **H** are mildly cytotoxic, whereas **A**, **J**, and **K** are slightly cytostatic (Table 1; Figure 3A).

HCT-8 cells were infected with oocysts of *C. parvum* Iowa isolate and parasites proliferated ~15-fold over 48 hr as measured by quantitative real-time PCR (Figure 3B). Parasites were also quantified using a biotin-conjugated VVL lectin that specifically recognizes sporozoites and intracellular stages but not the outer oocyst wall (see Experimental Procedures) (Gut and Nelson, 1999b; Hashim et al., 2004, 2006; Winter et al., 2000). Paromomycin inhibited parasite growth with a value of EC_{50} = 120 μM, validating the assay (literature values of EC_{50} = 65–130 μM; Perkins et al., 1998; Woods et al., 1995; You et al., 1996) (Figure S2). Compounds **A**, **F**, **G**, and **H** display significant dose-dependent antiparasitic activity in this assay (Table 1; Figure 3C). We confirmed the antiparasitic activity of **A**, **F**, **G**, and **H** using a real-time PCR assay that measures the abundance of parasite ribosomal RNA genes (Figure 3D) (Cai et al., 2005). No correlation exists between the antiparasitic activity of the compounds and cytotoxic/cytostatic effects, so the antiparasitic activities must result from direct effects on the parasite. These observations suggest that at least four compounds (**A**, **F**, **G**, and **H**) enter the parasite, which is a very important finding given that failure of drug uptake has been frequently invoked to explain the resistance of *Cryptosporidium* to antiparasitic drugs (Griffiths et al., 1998; Mead, 2002).

SIGNIFICANCE

***C. parvum* is an important pathogen of both the developed and developing world and a potential biowarfare agent. This protozoan parasite has eluded drug treatment and no**

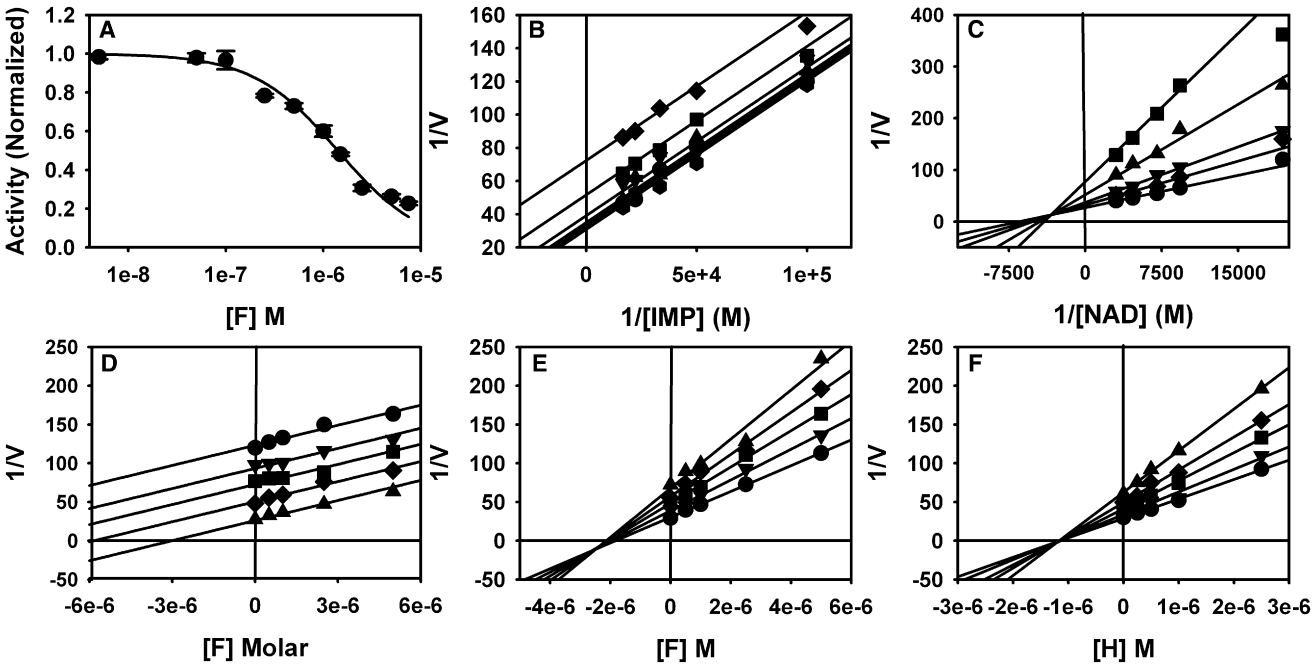

Figure 2. Inhibitor Characterization

(A) IC_{50} determination for compound **F**.

(B) The mechanism of inhibition for compound **F** versus IMP, [**F**] = ⬢ 0.0 μM; ▼ 0.5 μM; ▲ 1.0 μM; ■ 2.5 μM; ◆ 5.0 μM.

(C) The mechanism of inhibition for compound **F** versus NAD^+, [**F**] = ● 0.0 μM; ◆ 0.5 μM; ▼ 1.0 μM; ▲ 2.5 μM; ■ 5.0 μM.

(D) Dual-inhibitor experiments for compound **F** versus tiazofurin, [tiazofurin] = ● 0.0 mM; ▼ 2.0 mM; ■ 4.0 mM; ◆ 6.0 mM; ▲ 8.0 mM.

(E) Dual-inhibitor experiments for compound **F** versus ADP, [ADP] = ● 0.0 mM; ▼ 5.0 mM; ■ 10.0 mM; ◆ 15.0 mM; ▲ 20.0 mM.

(F) Dual-inhibitor experiments for compound **H** versus ADP, [ADP] = ● 0.0 mM; ▼ 5.0 mM; ■ 10.0 mM; ◆15.0 mM; ▲ 20.0 mM.

Conditions as described in Experimental Procedures.

vaccines exist. Eukaryotic pathogens present a particularly challenging problem for drug design because the targets generally bear a close resemblance to host proteins. Surprisingly, the purine salvage pathway of *C. parvum* relies on an IMPDH likely obtained from a prokaryote through horizontal gene transfer, and thus is very different from the host counterpart (Striepen et al., 2002, 2004). We designed an HTS to target the highly diverged NAD site by exploiting our detailed understanding of the kinetic mechanism of *C. parvum* IMPDH. This screen identified ten parasite-selective inhibitors, all of which bind in the NAD site as designed. Two different classes of interactions are observed: five compounds bind only in the nicotinamide portion of the NAD site, whereas three extend from the nicotinamide site into the adenosine subsite. Four compounds display antiparasitic activity in a cell-culture model of infection, further validating the choice

Table 2. Mechanism of Inhibition

	Versus IMP (UC)	Versus NAD^+ (NC)		Dual-Inhibitor Analysis α	
Inhibitor	K_{ii} (μM)	E•IMP K_{is} (μM)	E-XMP* K_{ii} (μM)	Tiazofurin	ADP
A	5.6 ± 0.5	3 ± 2	4 ± 2	∞ (ME)	1.3 (I)
B	2.7 ± 0.2	1.7 ± 0.6	2.5 ± 1.2	∞ (ME)	0.6 (S)
C	1.5 ± 0.1	1.5 ± 0.7	1.4 ± 0.2	∞ (ME)	0.3 (S)
D	4.5 ± 0.4	1.8 ± 0.5	7 ± 4	∞ (ME)	0.7 (S)
E	1.0 ± 0.1	4.1 ± 2.0	1.5 ± 0.3	∞ (ME)	2.7 (A)
F	3.7 ± 0.4	1.4 ± 0.2	2.7 ± 0.6	∞ (ME)	2.0 (A)
G	0.17 ± 0.01	0.14 ± 0.04	0.20 ± 0.05	n.d.	n.d.
H	0.61 ± 0.02	1.3 ± 0.4	1.1 ± 0.4	∞ (ME)	0.8 (I)
J	11.4 ± 0.3	4.1 ± 0.2	15 ± 3	∞ (ME)	0.6 (S)

Nomenclature of Cleland (1963), where noncompetitive (mixed) inhibition is described by two inhibition constants, K_{is} and K_{ii}. In the present case, K_{is} and K_{ii} describe the affinity of the inhibitor for the E•IMP and E-XMP* complexes, respectively. UC, uncompetitive; NC, noncompetitive; ME, mutually exclusive; I, independent; S, synergistic; A, antagonistic. n.d., not determined.

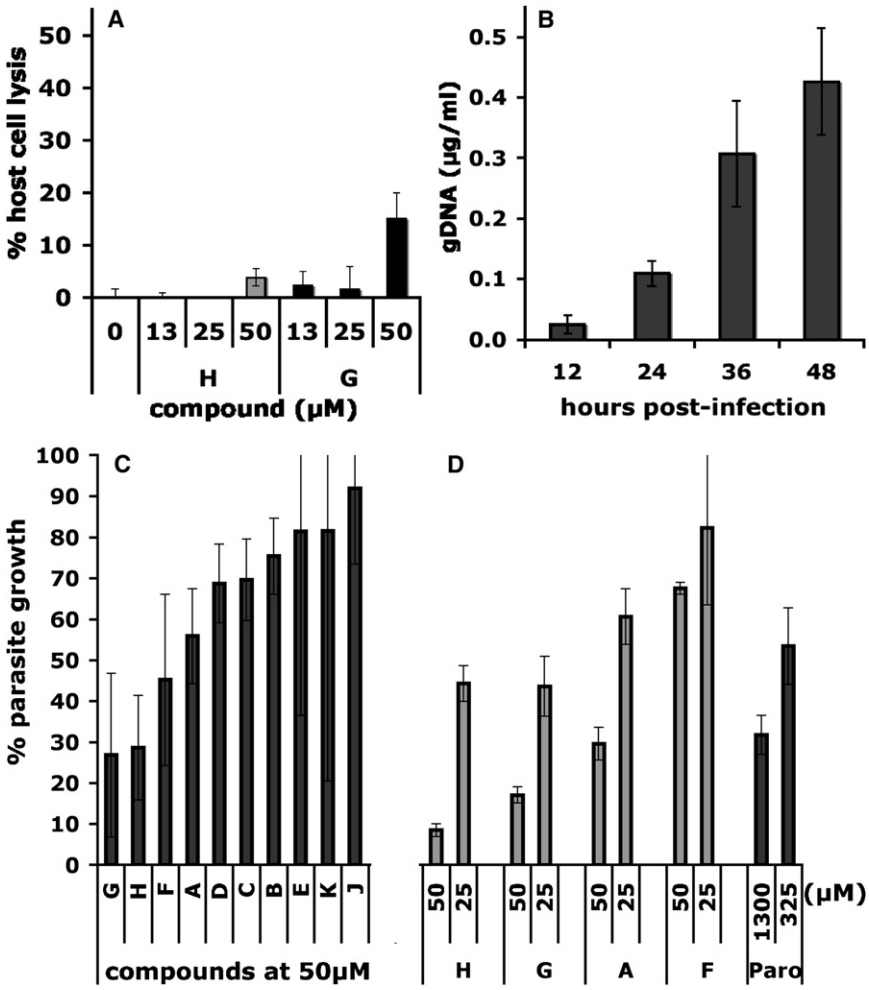

Figure 3. Activity of the Principal Hits in a Cell-Culture Model of *Cryptosporidium* Infection

(A) Representative cytotoxicity assay showing the cytolytic effects of compounds **G** and **H** monitored by the release of lactate dehydrogenase (LDH).

(B) Parasite proliferation as measured by real-time PCR over 48 hr, the period over which the antiparasitic effects of compounds **A**–**K** were determined.

(C) VVL-ELISA *C. parvum* growth assay.

(D) Real-time PCR *C. parvum* growth assay. Assays as described in Experimental Procedures. The error bars represent the standard deviation. Paro, paromomycin.

of IMPDH as target against cryptosporidiosis. Importantly, our inhibitors are already more potent than paromomycin, the current gold standard for anticryptosporidial activity.

EXPERIMENTAL PROCEDURES

Materials

The compound collections were provided by the National Screening Laboratory for the Regional Centers of Excellence in BioDefense and Emerging Infectious Disease (NSRB) at Harvard Medical School. The initial screen included 44,522 compounds from the following libraries: ActiMol TimTec 1, Bionet 2, ChemDiv 2, ChemDiv 3, Maybridge 4, NINDS custom collection, SpecPlus collection, BIOMOL ICCB known bioactives, ICBG 1 fungal extracts, and Starr Foundation extracts 1. Compounds **D**, **E**, **F**, **G**, **H**, and **L** were purchased from ChemDiv (San Diego, CA, USA), **K** from TimTec (Newark, DE, USA), and **J** from Asinex Ltd. (Moscow, Russia). Compounds **A**, **B**, and **C** were synthesized as described in the Supplemental Data. *C. parvum* oocysts of the Iowa strain were a kind gift from Dr. J. R. Mead (Emory University). VVL-biotin was purchased from Vector Labs (Burlingame, CA, USA).

Enzyme Purification and Assays

Recombinant human IMPDH1 and IMPDH2 and *C. parvum* were expressed in *guaB* strains of *Escherichia coli* (which lack endogenous IMPDH) and purified as described previously (Farazi et al., 1997; Mortimer and Hedstrom, 2005; Umejiego et al., 2004). Assays were routinely performed in 50 mM Tris-HCl (pH 8.0), 100 mM KCl, 3 mM EDTA, and 1 mM dithiothreitol (assay buffer) at 25°C. The production of NADH was monitored by following changes in absorbance or fluorescence.

Primary Screen

Table S2 describes the assay protocol. Assays were performed in duplicate in 384-well, clear flat bottom polystyrene nonbinding surface microplates (Corning 3640). Inhibitors (100 nl) were added to 30 μl of enzyme solution. An initial absorbance measurement at 340 nm was obtained using an Envision plate reader, and the reaction was initiated by the addition of IMP and NAD (40 μl) to give final assay conditions: 250 μM IMP, 500 μM NAD, and 70 nM *C. parvum* IMPDH in assay buffer. The reaction proceeded for ~3 hr, then was quenched by the addition of GMP (10 μl, final concentration 25 mM). The absorbance at 340 nm was measured, and the change in absorbance was determined by subtracting the initial value. Positive (12–25 mM GMP) and negative (no inhibitor) controls were included on each plate. This screen identified 134 compounds that displayed >45% inhibition with z scores ≤ -10.

Inhibitor Characterization

The values of K_i with respect to NAD^+ were determined using a saturating IMP concentration (150 μM; K_m = 29 μM; Umejiego et al., 2004) and varied NAD^+ concentrations. The values of K_i with respect to IMP were determined by using a fixed NAD^+ concentration (500 μM; K_m = 150 μM; Umejiego et al., 2004). The mechanism of inhibition was determined by the fit to the appropriate equation for uncompetitive or noncompetitive inhibition (Cleland, 1963). Dual-inhibition experiments with tiazofurin and ADP were performed with constant concentrations of IMP (250 μM) and NAD^+ (250 μM). Data were fit to an equation describing multiple inhibition (Equation 1),

$$v = v_0/(1 + [I]/K_i + [J]/K_j + [I][J]/\alpha K_i K_j), \quad (1)$$

where I and J are the inhibitors, v_0 is the initial velocity in the absence of inhibitors, α is the interaction constant, and K_i and K_j are the inhibition constants of I and J, respectively. Values of $\alpha > 8000$ were assigned as ∞. Detailed protocols are provided in the Supplemental Data.

Cell-Culture Model of *C. parvum* Infection

The human ileocecal adenocarcinoma epithelial cell line, HCT-8, was used to support *C. parvum* infection in vitro. Oocysts were treated with 10 mM HCl to facilitate excystation (Gut and Nelson, 1999a) and applied to an HCT-8 monolayer. Parasites were measured with biotin-conjugated VVL (Vector Labs, Burlingame, CA, USA) in a cell-based ELISA adapted to a 96-well format (Gut and Nelson, 1999b; Moriarty et al., 2005), or by real-time PCR as

described by Cai et al. (2005). Detailed protocols are provided in the Supplemental Data.

Effects of the Compounds on the Host Cells

The cytotoxic and cytostatic effects of compounds **A**–**K** on HCT-8 cells were determined using the CytoTox96 assay (Promega, Madison, WI, USA) and the LIVE/DEAD assay (Molecular Probes, Carlsbad, CA, USA).

Supplemental Data

Supplemental Data include two figures, two tables, Supplemental Experimental Procedures, and Supplemental References and can be found with this article online at http://www.chembiol.com/cgi/content/full/15/1/70/DC1/.

ACKNOWLEDGMENTS

This work was supported by NIH RO1 AI055268 (B.S.). Facilities and compound libraries for high-throughput screening were made available through the National Screening Laboratory for the Regional Centers of Excellence in BioDefense and Emerging Infectious Disease (NSRB/NERCE). We thank members of the NSRB and ICCB-Longwood (Harvard Medical School) for their ongoing assistance. Molecular graphics images were produced using the UCSF Chimera package from the Resource for Biocomputing, Visualization, and Informatics at the University of California, San Francisco (supported by NIH P41 RR-01081).

Received: October 5, 2007
Revised: December 7, 2007
Accepted: December 17, 2007
Published: January 25, 2008

REFERENCES

Abrahamsen, M.S., Templeton, T.J., Enomoto, S., Abrahante, J.E., Zhu, G., Lancto, C.A., Deng, M., Liu, C., Widmer, G., Tzipori, S., et al. (2004). Complete genome sequence of the apicomplexan, *Cryptosporidium parvum*. Science *304*, 441–445.

Abubakar, I., Aliyu, S.H., Arumugam, C., Usman, N.K., and Hunter, P.R. (2007). Treatment of cryptosporidiosis in immunocompromised individuals: systematic review and meta-analysis. Br. J. Clin. Pharmacol. *63*, 387–393.

Arrowood, M.J. (2002). In vitro cultivation of *Cryptosporidium* species. Clin. Microbiol. Rev. *15*, 390–400.

Berkman, D.S., Lescano, A.G., Gilman, R.H., Lopez, S.L., and Black, M.M. (2002). Effects of stunting, diarrhoeal disease, and parasitic infection during infancy on cognition in late childhood: a follow-up study. Lancet *359*, 564–571.

Cai, X., Woods, K.M., Upton, S.J., and Zhu, G. (2005). Application of quantitative real-time reverse transcription-PCR in assessing drug efficacy against the intracellular pathogen *Cryptosporidium parvum* in vitro. Antimicrob. Agents Chemother. *49*, 4437–4442.

Carey, C.M., Lee, H., and Trevors, J.T. (2004). Biology, persistence and detection of *Cryptosporidium parvum* and *Cryptosporidium hominis* oocyst. Water Res. *38*, 818–862.

Cleland, W.W. (1963). The kinetics of enzyme-catalyzed reactions with two or more substrates or products. II. Inhibition: nomenclature and theory. Biochim. Biophys. Acta *67*, 173–187.

Corso, P.S., Kramer, M.H., Blair, K.A., Addiss, D.G., Davis, J.P., and Haddix, A.C. (2003). Cost of illness in the 1993 waterborne *Cryptosporidium* outbreak, Milwaukee, Wisconsin. Emerg. Infect. Dis. *9*, 426–431.

Digits, J.A., and Hedstrom, L. (1999). Kinetic mechanism of *Tritrichomonas foetus* inosine-5′-monophosphate dehydrogenase. Biochemistry *38*, 2295–2306.

DuPont, H.L., Chappell, C.L., Sterling, C.R., Okhuysen, P.C., Rose, J.B., and Jakubowski, W. (1995). The infectivity of *Cryptosporidium parvum* in healthy volunteers. N. Engl. J. Med. *332*, 855–859.

Farazi, T., Leichman, J., Harris, T., Cahoon, M., and Hedstrom, L. (1997). Isolation and characterization of mycophenolic acid resistant mutants of inosine 5′-monophosphate dehydrogenase. J. Biol. Chem. *272*, 961–965.

Fayer, R. (2004). *Cryptosporidium*: a water-borne zoonotic parasite. Vet. Parasitol. *126*, 37–56.

Griffiths, J.K., Balakrishnan, R., Widmer, G., and Tzipori, S. (1998). Paromomycin and geneticin inhibit intracellular *Cryptosporidium parvum* without trafficking through the host cell cytoplasm: implications for drug delivery. Infect. Immun. *66*, 3874–3883.

Gut, J., and Nelson, R.G. (1999a). *Cryptosporidium parvum*: lectins mediate irreversible inhibition of sporozoite infectivity in vitro. J. Eukaryot. Microbiol. *46*, 48S–49S.

Gut, J., and Nelson, R.G. (1999b). *Cryptosporidium parvum*: synchronized excystation in vitro and evaluation of sporozoite infectivity with a new lectin-based assay. J. Eukaryot. Microbiol. *46*, 56S–57S.

Hashim, A., Clyne, M., Mulcahy, G., Akiyoshi, D., Chalmers, R., and Bourke, B. (2004). Host cell tropism underlies species restriction of human and bovine *Cryptosporidium parvum* genotypes. Infect. Immun. *72*, 6125–6131.

Hashim, A., Mulcahy, G., Bourke, B., and Clyne, M. (2006). Interaction of *Cryptosporidium hominis* and *Cryptosporidium parvum* with primary human and bovine intestinal cells. Infect. Immun. *74*, 99–107.

Hedstrom, L., and Gan, L. (2006). IMP dehydrogenase: structural schizophrenia and an unusual base. Curr. Opin. Chem. Biol. *10*, 520–525.

Hedstrom, L., Cheung, K., and Wang, C.C. (1990). A novel mechanism of mycophenolic acid resistance in the protozoan parasite *Tritrichomonas foetus*. Biochem. Pharmacol. *39*, 151–160.

Huang, D.B., and White, A.C. (2006). An updated review on *Cryptosporidium* and *Giardia*. Gastroenterol. Clin. North Am. *35*, 291–314.

Huang, D.B., Chappell, C., and Okhuysen, P.C. (2004). Cryptosporidiosis in children. Semin. Pediatr. Infect. Dis. *15*, 253–259.

Mead, J.R. (2002). Cryptosporidiosis and the challenges of chemotherapy. Drug Resist. Updat. *5*, 47–57.

Moriarty, E.M., Duffy, G., McEvoy, J.M., Caccio, S., Sheridan, J.J., McDowell, D., and Blair, I.S. (2005). The effect of thermal treatments on the viability and infectivity of *Cryptosporidium parvum* on beef surfaces. J. Appl. Microbiol. *98*, 618–623.

Mortimer, S.E., and Hedstrom, L. (2005). Autosomal dominant retinitis pigmentosa mutations in inosine 5′-monophosphate dehydrogenase type I disrupt nucleic acid binding. Biochem. J. *390*, 41–47.

Perkins, M.E., Wu, T.W., and Le Blancq, S.M. (1998). Cyclosporin analogs inhibit in vitro growth of *Cryptosporidium parvum*. Antimicrob. Agents Chemother. *42*, 843–848.

Pettersen, E.F., Goddard, T.D., Huang, C.C., Couch, G.S., Greenblatt, D.M., Meng, E.C., and Ferrin, T.E. (2004). UCSF Chimera—a visualization system for exploratory research and analysis. J. Comput. Chem. *25*, 1605–1612.

Ratcliffe, A.J. (2006). Inosine 5′-monophosphate dehydrogenase inhibitors for the treatment of autoimmune diseases. Curr. Opin. Drug Discov. Dev. *9*, 595–605.

Striepen, B., White, M.W., Li, C., Guerini, M.N., Malik, S.B., Logsdon, J.M., Jr., Liu, C., and Abrahamsen, M.S. (2002). Genetic complementation in apicomplexan parasites. Proc. Natl. Acad. Sci. USA *99*, 6304–6309.

Striepen, B., Pruijssers, A.J., Huang, J., Li, C., Gubbels, M.J., Umejiego, N.N., Hedstrom, L., and Kissinger, J.C. (2004). Gene transfer in the evolution of parasite nucleotide biosynthesis. Proc. Natl. Acad. Sci. USA *101*, 3154–3159.

Templeton, T.J., Iyer, L.M., Anantharaman, V., Enomoto, S., Abrahante, J.E., Subramanian, G.M., Hoffman, S.L., Abrahamsen, M.S., and Aravind, L. (2004). Comparative analysis of apicomplexa and genomic diversity in eukaryotes. Genome Res. *14*, 1686–1695.

Umejiego, N.N., Li, C., Riera, T., Hedstrom, L., and Striepen, B. (2004). *Cryptosporidium parvum* IMP dehydrogenase: identification of functional, structural and dynamic properties that can be exploited for drug design. J. Biol. Chem. *279*, 40320–40327.

Upton, S.J. (1997). In vitro cultivation. In *Cryptosporidium* and Cryptosporidiosis, R. Fayer, ed. (Boca Raton, FL: CRC Press), pp. 181–207.

Winter, G., Gooley, A.A., Williams, K.L., and Slade, M.B. (2000). Characterization of a major sporozoite surface glycoprotein of *Cryptosporidium parvum*. Funct. Integr. Genomics *1*, 207–217.

Woods, K.M., Nesterenko, M.V., and Upton, S.J. (1995). Development of a microtitre ELISA to quantify development of *Cryptosporidium parvum* in vitro. FEMS Microbiol. Lett. *128*, 89–94.

Xu, P., Widmer, G., Wang, Y., Ozaki, L.S., Alves, J.M., Serrano, M.G., Puiu, D., Manque, P., Akiyoshi, D., Mackey, A.J., et al. (2004). The genome of *Cryptosporidium hominis*. Nature *431*, 1107–1112.

You, X., Arrowood, M.J., Lejkowski, M., Xie, L., Schinazi, R.F., and Mead, J.R. (1996). A chemiluminescence immunoassay for evaluation of *Cryptosporidium parvum* growth in vitro. FEMS Microbiol. Lett. *136*, 251–256.